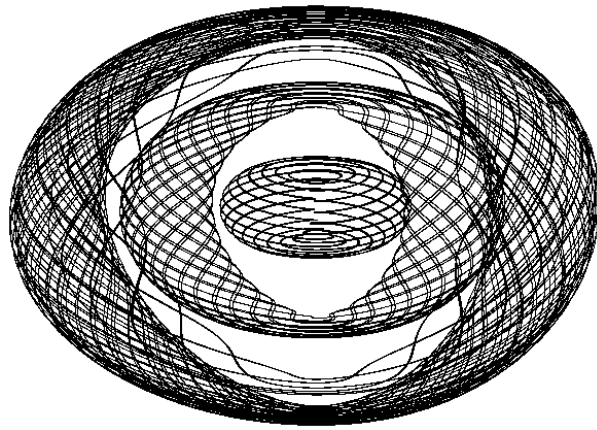


MODELS AND NUMERICAL METHODS FOR PHYSICS

EXAMINATION PROJECT



Federico Magnani
NOVEMBER 2020

Contents

1	The Competitive Lotka Volterra system with logistic growth	3
1.1	Introduction to the method	3
1.2	Introduction to the Lotka Volterra system	4
1.3	Two competing populations with logistic growth	7
2	The Stroboscopic Map applied to a Lotka Volterra system with time-periodic perturbation	13

Introduction

This work can be divided into two main sections. Both aim to study a dynamical system, but with different methods. In the first section mainly an analytical study is performed, while in the second case almost only numerical methods are involved. Ideally the best solution is to merge and complement mutually the two approaches, but the division here made is useful to underline the advantages and the weaknesses of both.

Chapter 1

The Competitive Lotka Volterra system with logistic growth

In this section a purely analytical study of a variation of the so called Lotka Volterra system will be performed. After a brief introduction to the method and to the model, the full analysis of the Two Competing Preys with Logistic Growth case is made, exploiting two different yet strongly connected approaches: the study of the evolution flow and the study of the Lyapunov function.

1.1 Introduction to the method

In the following, we will treat the systems from a dynamical point of view, studying the evolution flow in the phase space defined as:

$$\Phi(\mathbf{x}(t)) := \begin{pmatrix} \dot{x}_1 \\ \dot{x}_2 \\ \dots \\ \dot{x}_d \end{pmatrix} = \frac{d}{dt}\mathbf{x}(t) \quad (1.1)$$

where Φ is a vectorial field from \mathbb{R}^d to \mathbb{R}^d . For each initial condition \mathbf{x}_0 a trajectory $\mathbf{x}(t)$ in the phase space \mathbb{R}^d represents the solution to the ordinary differential equation (1.1).

The notation underlies a system of d differential equation of the form

$$\Phi_i(x_1(t), x_2(t), \dots, x_d(t)) = \frac{d}{dt}x_i(t) \quad (1.2)$$

and evolutions corresponding to differential equations of order greater than one can always be reconducted to this fundamental case, at the cost of increasing the dimensionality

of the system.

The evolution flow Φ may explicitly depend on time t . In such a case the dimensionality of the system is increased by one, since we can treat time as a spatial coordinate with constant derivative, i.e. we can add to the components of \mathbf{x} and Φ respectively $x_0 \equiv t$ and $\Phi_0 = \dot{x}_0 = 1$.

A reduction of the dimensionality is allowed by the existence of a first integral $H(\mathbf{x})$ defined as a function $\mathbb{R}^d \mapsto \mathbb{R}$ whose gradient is orthogonal to Φ , i.e $\text{grad } H \cdot \Phi = 0$.

In such a case, the relation

$$\dot{H}(\mathbf{x}) = \sum_{i=1}^d \frac{\partial H}{\partial x_i} \dot{x}_i = \text{grad } H \cdot \Phi \equiv 0 \quad (1.3)$$

shows that H is stationary along each trajectory, i.e. $H(\mathbf{x}_0) = H(\mathbf{x}(t)) \equiv E \forall t$. The solutions $\mathbf{x}(t)$ of equation (1.1) are implicitly defined by $H(\mathbf{x}) = E$.

The analysis of the system is usually performed determining the stationary points, for which $\Phi(x)=0$, and their stability. This immediately gives the picture of the main features of the evolution flow. In this regard it is useful to introduce the Lyapunov function $\phi(\mathbf{x}) \mathbb{R}^d \mapsto \mathbb{R}$, defined by the two conditions:

$$\text{i) } \text{grad } \phi \cdot \Phi \leq 0$$

$$\text{ii) } \phi(x_*)=0, \phi(x \neq x_*) > 0 \quad (\phi \text{ has a minimum in } \mathbf{x}_*)$$

where \mathbf{x}_* is a specified equilibrium point for $\Phi(\mathbf{x})$. If the Lyapunov function exists, \mathbf{x}_* is an attractive fixed point.

1.2 Introduction to the Lotka Volterra system

The original Lotka Volterra system has been proposed in the early 1900s in the field of population dynamics. Being a very simple yet powerful model, since that time many generalizations and variations have been developed. We will summarize briefly the properties of the original system, called Predator Prey, then study in more detail the case of the Competitive Preys.

The name refers to the ecological interpretation in which two species interact, one as a predator and the other as a prey. The system, made up of two ordinary non linear differential equations, is usually formulated in the following way:

$$\dot{x} := \frac{dx}{dt} = \alpha x - \gamma xy \quad (1.4)$$

$$\dot{y} := \frac{dy}{dt} = -\beta y + \delta xy \quad (1.5)$$

where \dot{x} and \dot{y} are the instantaneous growth rate of the two populations. α represents the natural birth rate of the preys, while γ represents their predation rate. If we interpret xy as the probability for a prey and a predator to meet and interact, γ can be read as the fraction of times in which the prey is actually caught. Overall, the change over time of the number of the preys is given by the balance between the rate at which they're born and the rate at which they're predated.

Simmetrically β is the natural death rate of the predators, that are supposed to die if no predation occurs, while δ is their hunting efficiency. Note that γ and δ are different costants, since the gain percieved by predators can differ from the loss percieved by the preys.

Scaling the coordinates as $x \mapsto \delta x$ $y \mapsto \gamma y$, the evolution flow can be defined as:

$$\Phi(\mathbf{x}) = \begin{pmatrix} x(\alpha - y) \\ y(x - \beta) \end{pmatrix} \quad (1.6)$$

Dividing the first equation for x and second for y , the following change of coordinates looks natural:

$$X = \log(x) \quad Y = \log(y)$$

so to have

$$\dot{X} = \alpha - e^Y := \frac{dT(Y)}{dY} \quad (1.7)$$

$$\dot{Y} = e^X - \beta := -\frac{dV(X)}{dX} \quad (1.8)$$

from which we get as first integral

$$H = T(Y) + V(X) \quad (1.9)$$

$$= e^X + e^Y - \beta X - \alpha Y \quad (1.10)$$

$$\equiv x + y - \beta \log(x) - \alpha \log(y) \quad (1.11)$$

The representation of the system is shown in the figures (1.1), where the flow $\Phi(\mathbf{x})$ is numerically computed and plotted for both the coordinate forms.

We can recover analitically the features of the system shown in the figure (1.1, left) studying the fixed points of the evolution flow and their stability.

The equilibrium points \mathbf{x}_\star verify the condition $\Phi(\mathbf{x}_\star)=0$ and are found to be $\mathbf{x}_{0,0} = (0,0)$ and $\mathbf{x}_{+,+} = (\beta, \alpha)$. Their stability is studied linearizing the system around each of them through the matrix

$$\nabla \Phi = \begin{bmatrix} \frac{\partial \Phi_x}{\partial x} & \frac{\partial \Phi_x}{\partial y} \\ \frac{\partial \Phi_y}{\partial x} & \frac{\partial \Phi_y}{\partial y} \end{bmatrix} \quad (1.12)$$

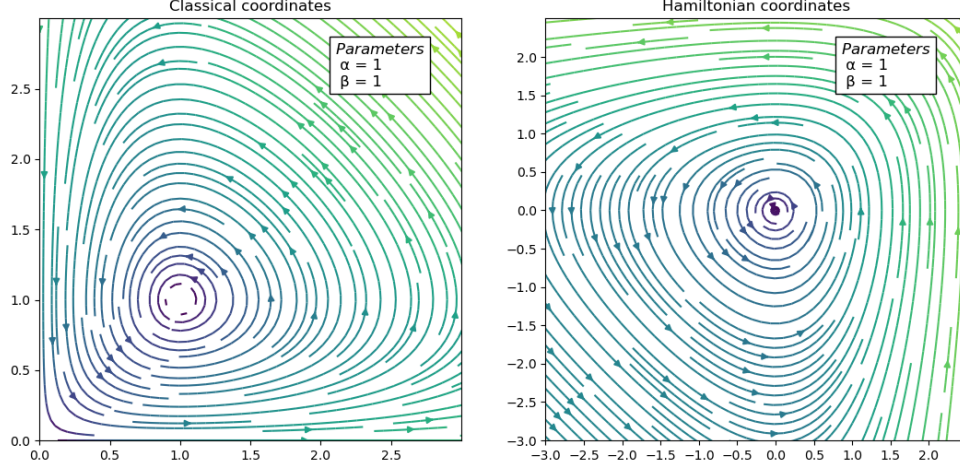


Figure 1.1: In the figure is represented the evolution flow $\Phi(\mathbf{x})$ computed numerically, in the classical representation (left) and in the hamiltonian form (right). Note the presence of a center in (β, α) .

If the eigenvalues λ of $\nabla\Phi(\mathbf{x})$ have all negative real part, that is a stable and attractive equilibrium. If the dimension of the phase space is even and all the eigenvalues are completely imaginary and complex conjugates, that is a center. This is the case of (β, α) . If one or more eigenvalues have positive real part, the equilibrium is unstable, and that's the case of $(0,0)$. We skip the detailed computation here, since an analogous study is shown below for a different scenario.

Considering equations (1.5), note that in absence of interaction the predators are assumed to die while the preys are assumed to grow exponentially and with no limit. A development of the system is to limit the natural resources for the preys, with a term quadratic in x representing the intraspecific competition for the food. The modified equations have the following form:

$$\dot{x} = \alpha x \left(1 - \frac{x}{x_\infty}\right) - xy \quad (1.13)$$

$$\dot{y} = -\beta y + xy \quad (1.14)$$

where x_∞ , called carrying capacity in ecology, directly represents the maximum number of preys that the ecosystem in absence of predators can feed at once. The kind of growth here modeled is called *logistic growth*. The equilibrium points are again $(0,0)$ and (β, α) but the latter is an attractive centrum.

1.3 Two competing populations with logistic growth

In this section the following system will be studied:

$$\dot{x} = \Phi_x \equiv x(a - y) - k_1x(x - b) \quad (1.15)$$

$$\dot{y} = \Phi_y \equiv y(b - x) - k_2y(y - a) \quad (1.16)$$

that can be interpreted as an ecological system with two preys in competition with logistic growth, as shown by the parameter substitution

$$\alpha_1 = a + bk_1, \quad x_{\infty,1} = \alpha_1/k_1$$

$$\alpha_2 = b + ak_2, \quad x_{\infty,2} = \alpha_2/k_2$$

The study we perform will exploit two different approaches: the analysis of the stability of the fixed points of $\Phi(\mathbf{x})$ and the analysis of the Lyapunov function $\phi(\mathbf{x})$ that will be derived.

Setting $\Phi(\mathbf{x}_*)=0$ the following equilibria are found:

$$\mathbf{x}_{00} = (0,0)$$

$$\mathbf{x}_{0+} = (0, a + \frac{b}{k_2})$$

$$\mathbf{x}_{+0} = (b + \frac{a}{k_1}, 0)$$

$$\mathbf{x}_{++} = (b,a) \quad \text{if } k_1k_2 \neq 1$$

The first three equilibria are straightforward to derive, while the fourth depends on the relation between k_1 and k_2 since, given that x and $y \neq 0$, it is

$$(a - y_*) - k_1(x_* - b) = 0 \quad (1.17)$$

$$(b - x_*) - k_2(y_* - a) = 0 \quad (1.18)$$

Such a system represents the intersection between two lines with angular coefficient $\frac{\Delta y}{\Delta x}$ equal to k_1 and $\frac{1}{k_2}$ respectively. If $k_1k_2 = 1$ the two lines collapse into the same and the whole set $y - a = k_1(x - b)$ is stationary for $\Phi(\mathbf{x})$.

In figures (1.2) the flow $\Phi(\mathbf{x})$ in phase space is shown for the two cases k_1k_2 greater or smaller than 1, and the equilibrium points are indicated. Their stability can be guessed from the pictures, but we will now derive it in an analytical way. In the plots and in all the following, for the sake of simplicity, we will assume $a=b=1$.

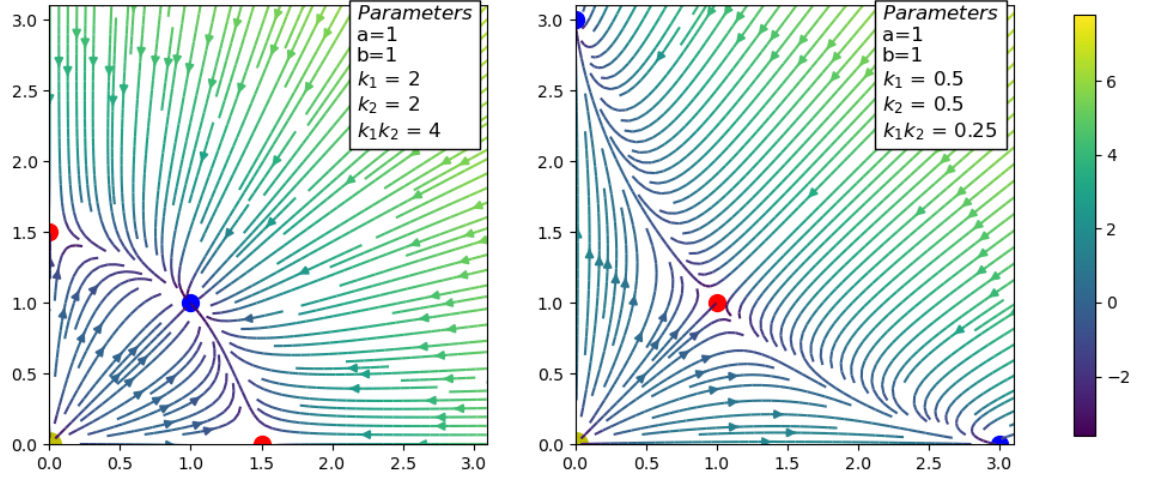


Figure 1.2: In the figures is represented the evolution flow $\Phi(\mathbf{x})$ computed numerically, for different choices of the parameters. The equilibrium points are indicated; with yellow for unstable nodes, blue for attractive nodes, red for saddles. The color bar has arbitrary units.

The linearized evolution is defined locally by the matrix $\nabla\Phi$ whose component are:

$$\frac{\partial\Phi_x}{\partial x} = (a - y) - 2k_1x + k_1b \quad (1.19)$$

$$\frac{\partial\Phi_x}{\partial y} = -x \quad (1.20)$$

$$\frac{\partial\Phi_y}{\partial x} = -y \quad (1.21)$$

$$\frac{\partial\Phi_y}{\partial y} = (b - x) - 2k_2y + k_2a \quad (1.22)$$

$$(1.23)$$

Thus for \mathbf{x}_{00} we have

$$\nabla\Phi(0,0) = \begin{bmatrix} a + k_1b & 0 \\ 0 & b + k_2a \end{bmatrix} \quad (1.24)$$

and since all the parameters are defined to be positive, that's an unstable node. For small displacements in any direction the evolution diverges from the origin.

For \mathbf{x}_{0+} we have

$$\nabla\Phi(0, 1 + \frac{1}{k_2}) = \begin{bmatrix} k_1 - \frac{1}{k_2} & 0 \\ -(1 + \frac{1}{k_2}) & -(1 + k_2) \end{bmatrix} \quad (1.25)$$

The local evolution can be expressed

$$\nabla\Phi_{\mathbf{x}_{0+}}(\Delta x, \Delta y) = [\frac{k_1k_2 - 1}{k_1k_2}\Delta x]\hat{\mathbf{x}} - [(1 + \frac{1}{k_2})\Delta x + (1 + k_2)\Delta y]\hat{\mathbf{y}} \quad (1.26)$$

or

$$\frac{d}{dt}\Delta x = \frac{d}{dt}(x - x_*) = \frac{k_1k_2 - 1}{k_1k_2}\Delta x \quad (1.27)$$

$$\frac{d}{dt}\Delta y = \frac{d}{dt}(y - y_*) = -(1 + \frac{1}{k_2})\Delta x + (1 + k_2)\Delta y \quad (1.28)$$

where the displacement $\Delta\mathbf{x}=(\mathbf{x}-\mathbf{x}_*)=\mathbf{x}$ can only be positive, since the populations are bounded to positive values. So along the $\hat{\mathbf{x}}$ direction, the flow contracts the displacement for $k_1k_2 < 1$ and diverges for $k_1k_2 > 1$. Along the $\hat{\mathbf{y}}$ direction the flow is in any case attractive onto the line

$$\Delta y = -\frac{1 + \frac{1}{k_2}}{1 + k_2}x \quad (1.29)$$

that connects \mathbf{x}_{0+} and \mathbf{x}_{+0} . Thus the stability of the equilibrium depends only on k_1k_2 being smaller than 1 (attractive equilibrium) or greater than 1 (saddle point). If $k_1k_2 = 0$ one of the eigenvalues is 0 and the whole line (1.29) is stationary, each of its points being an equilibrium point.

The case of \mathbf{x}_{+0} is symmetrical, while for \mathbf{x}_{++} we have

$$\nabla\Phi(b, a) = \begin{bmatrix} -k_1b & -b \\ -a & -k_2a \end{bmatrix} = \begin{bmatrix} -k_1 & -1 \\ -1 & -k_2 \end{bmatrix} \quad (1.30)$$

To simplify the computations let's consider the case $k_1 = k_2 = k$. The eigenvalue equation is $(-k - \lambda)^2 = 1$ from which

$$\lambda_{\pm} = \pm 1 - k \quad (1.31)$$

λ_- is always negative while λ_+ is positive for $k < 1$ (\mathbf{x}_{++} is a saddle point), negative for $k > 1$ (\mathbf{x}_{++} is an attractive node).

This completes the analytic study of the system. In the following an alternative approach is presented.

A so called gradient system is characterized by an evolution flow $\Phi(\mathbf{x})$ that can be expressed through the gradient of a suitable scalar field $\phi(\mathbf{x})$ as $\Phi(\mathbf{x}) = -\nabla\phi(\mathbf{x})$. In such a case $\phi(\mathbf{x})$ is a *hamiltonian function*, and the following conditions are satisfied:

$$\text{i) } \nabla\phi(\mathbf{x}) \cdot \Phi(\mathbf{x}) = -\nabla\phi(\mathbf{x}) \cdot \nabla\phi(\mathbf{x}) = 0$$

$$\text{ii) } \dot{\phi}(\mathbf{x}) = \nabla\phi(\mathbf{x})\dot{\mathbf{x}} = \nabla\phi(\mathbf{x}) \cdot \Phi(\mathbf{x}) = 0$$

$$\text{iii) } \nabla \times \Phi(\mathbf{x}) = 0$$

A direct consequence of condition (ii) is that the trajectories in the phase space can be seen as level curves of ϕ since $\dot{\phi}(\mathbf{x}(t)) = 0 \quad \forall t$.

The system here under consideration is not a gradient system, as we immediately have (recalling equations (1.23))

$$\nabla \times \Phi(\mathbf{x}) = \frac{\partial\Phi_y}{\partial x} - \frac{\partial\Phi_x}{\partial y} = x - y \quad (1.32)$$

A generalized gradient system is defined by a weaker set of conditions:

$$\text{i) } \nabla\phi(\mathbf{x}) \cdot \Phi(\mathbf{x}) \leq 0$$

$$\text{ii) } \dot{\phi}(\mathbf{x}) = \nabla\phi(\mathbf{x})\dot{\mathbf{x}} = \nabla\phi(\mathbf{x}) \cdot \Phi(\mathbf{x}) \leq 0$$

$$\text{iii) } \nabla \times (\nabla\phi(\mathbf{x})) = 0$$

in which case ϕ is called *Lyapunov function* and for a specified equilibrium point \mathbf{x}_\star holds the following:

$$\phi(\mathbf{x}_\star) = 0, \quad \phi(\mathbf{x} \neq \mathbf{x}_\star) > 0 \quad (1.33)$$

It can be proven that a generalized gradient system can be expressed in the form

$$\Phi(\mathbf{x}) = \dot{\mathbf{x}} = -\mathbf{D}(\mathbf{x})\nabla\phi(\mathbf{x}) \quad (1.34)$$

where $\mathbf{D}(\mathbf{x})$ is a semi-positive definite and symmetric matrix. The equation can be reversed to

$$\nabla\phi(\mathbf{x}) = -\mathbf{A}(\mathbf{x})\Phi(\mathbf{x}) \quad (1.35)$$

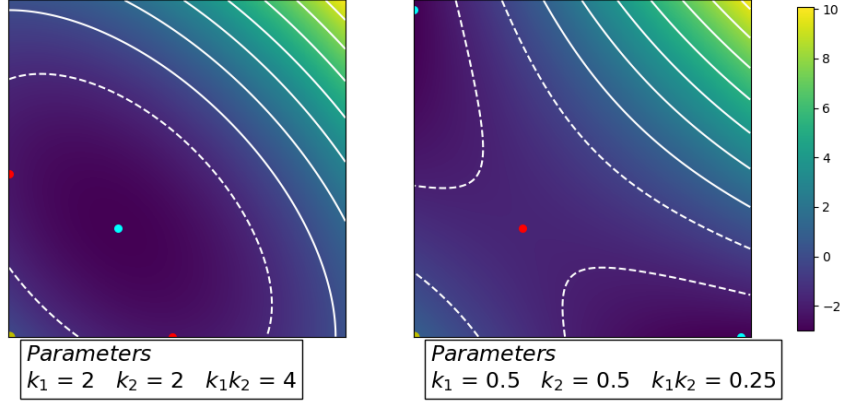


Figure 1.3: In the figures is represented the function $\phi(\mathbf{x})$ computed numerically, for the same choices of the parameters used in figures (1.2). The equilibrium points are indicated; with yellow for unstable nodes, cyan for attractive nodes, red for saddles. The color bar has arbitrary units.

that together with the conditions above allows to determine the function $\phi(\mathbf{x})$. Among the various choices of A the most simple is

$$A = \begin{bmatrix} \frac{1}{x} & 0 \\ 0 & \frac{1}{y} \end{bmatrix} \quad (1.36)$$

The proof that the conditions above hold is straightforward. Integrating the equations

$$\frac{\partial \phi}{\partial x} = -(a - y - k_1(x - b)) \quad (1.37)$$

$$\frac{\partial \phi}{\partial y} = -(b - x - k_2(y - a)) \quad (1.38)$$

we finally obtain the scalar function

$$\phi(\mathbf{x}) = -(a + k_1 b)x + \frac{k_1 x^2}{2} - (b + k_2 a)y + \frac{k_2 y^2}{2} + xy \quad (1.39)$$

In figures (1.3) $\phi(\mathbf{x})$ is shown for the same cases depicted in figures (1.2), and the the

fixed points are indicated. Again, it's easy to guess their stability from the picture, but let's now find analytically the same results.

In this regard, it is enough to study the behaviour of the hessian matrix of $\phi(\mathbf{x})$ computed at a specified point \mathbf{x}_\star , here \mathbf{x}_{++} .

It is

$$\frac{\partial^2 \phi}{\partial x^2} = k_1 \qquad \frac{\partial^2 \phi}{\partial y \partial x} = 1 \qquad (1.40)$$

$$\frac{\partial^2 \phi}{\partial x \partial y} = 1 \qquad \frac{\partial^2 \phi}{\partial y^2} = k_2 \qquad (1.41)$$

$$(1.42)$$

from which we immediately get the determinant as $\Delta = k_1 k_2 - 1$.

The three cases identified in the previous section are recovered as:

i $\Delta > 0 \quad k_1 k_2 > 1$

Condition that together with $\frac{\partial^2 \phi}{\partial x^2} > 0$ indicates that \mathbf{x}_{++} is a globally stable point, i.e. an attractive node.

ii $\Delta < 0 \quad k_1 k_2 < 1$

\mathbf{x}_{++} is a saddle point. As the system is bounded in the first quadrant, the two stable equilibriums \mathbf{x}_{0+} and \mathbf{x}_{+0} are defined.

iii $\Delta = 0 \quad k_1 k_2 = 1$

The whole line (1.29) is a minimum for $\phi(\mathbf{x})$.

This kind of stability analysis have been adapted to the system under consideration, from the article [Ying Tang, Ruoshi Yuan, Yi-An Ma, *Dynamical behaviors determined by the Lyapunov function in competitive Lotka-Volterra systems*, (Article in Physical Review E · January 2013)] available at <https://www.researchgate.net/publication/235627640>.

Chapter 2

The Stroboscopic Map applied to a Lotka Volterra system with time-periodic perturbation

In this section the analysis of a system perturbed by a time-periodic term will be performed, exploiting only numerical methods and in particular the so called Stroboscopic Map. A variety of figures will be derived and briefly described, using two similar yet very different maps, in order to give the idea of the power of such an approach to the system under consideration, and of the difficulties of the numerical integration.

Let's consider a variation of the Predator Prey system, slightly unbalanced in the following way:

$$\dot{x} = x(a^2 - y^2) \quad (2.1)$$

$$\dot{y} = y(x^2 - b^2) \quad (2.2)$$

The equilibrium points are unchanged and the Hamiltonian is easy to found, referring to equation (1.11). The system is autonomous, i.e. $\frac{\partial H}{\partial t} = 0$.

We will study in the following the previous system with a time-periodic perturbation as

$$\dot{x} = x(a^2 - y^2) + x\epsilon \cos \omega t \quad (2.3)$$

$$\dot{y} = y(x^2 - b^2) \quad (2.4)$$

that makes the system explicitly dependent on time. We can recover an autonomous description at the cost of increasing the dimensionality by one, defining a new variable $\theta(t) = \omega t$. The system has now the form

$$\dot{x} = x(a^2 - y^2) + x\epsilon \cos \theta \quad (2.5)$$

$$\dot{y} = y(x^2 - b^2) \quad (2.6)$$

$$\dot{\theta} = \omega \quad (2.7)$$

Some further transformations are useful. Noting that for $\epsilon = 0$ the system is Hamiltonian, we exploit the coordinate change $x \mapsto \log(x)$, $y \mapsto \log(y)$ and we then rescale the coordinates as $(x, y) \mapsto \frac{(x, y)}{2\pi}$ in order to have as a final form for the system:

$$\frac{\dot{x}}{2\pi} = (a^2 - e^{y/\pi}) + \epsilon \cos \theta \quad (2.8)$$

$$\frac{\dot{y}}{2\pi} = (e^{x/\pi} - b^2) \quad (2.9)$$

$$\dot{\theta} = \omega \quad (2.10)$$

The evolution flow

$$\Phi(\mathbf{x}(t)) = \begin{pmatrix} \dot{x} \\ \dot{y} \\ \dot{\theta} \end{pmatrix} \quad (2.11)$$

is an application $\mathbb{R}^3 \mapsto \mathbb{R}^3$.

The map used to numerically integrate the system is built on the top of the equation set (2.10) as

$$x_{n+1} = x_n + 2\pi\Delta t(a^2 - e^{y_{n+1}/\pi}) + \epsilon 2\pi\Delta t \cos \theta_n \quad (2.12)$$

$$y_{n+1} = y_n + 2\pi\Delta t(e^{x_n/\pi} - b^2) \quad (2.13)$$

$$\theta_{n+1} = \theta_n + \omega\Delta t = \theta_n + 2\pi\frac{\Delta t}{T} \quad (2.14)$$

where T is the period and $\omega = \frac{2\pi}{T}$. For $\epsilon = 0$ that's a symplectic integrator. A second map will be used later, in which the transformation $\theta = \omega t$ is not applied.

In the figures (2.1) the case for $\epsilon = 0$ is shown. Since perturbation is absent that's in fact a 2D map whose representation is given on the figure on the right. Anyway the evolution along θ is shown in the figure on the left, since that's the general workframe for the 3D system.

The main tool of our analysis will be the stroboscopic map. In the original system the forcing is periodic in time and then we added the θ coordinate in order to get rid of the explicit time dependence. Anyway we project the evolution in \mathbb{R}^3 onto the xy

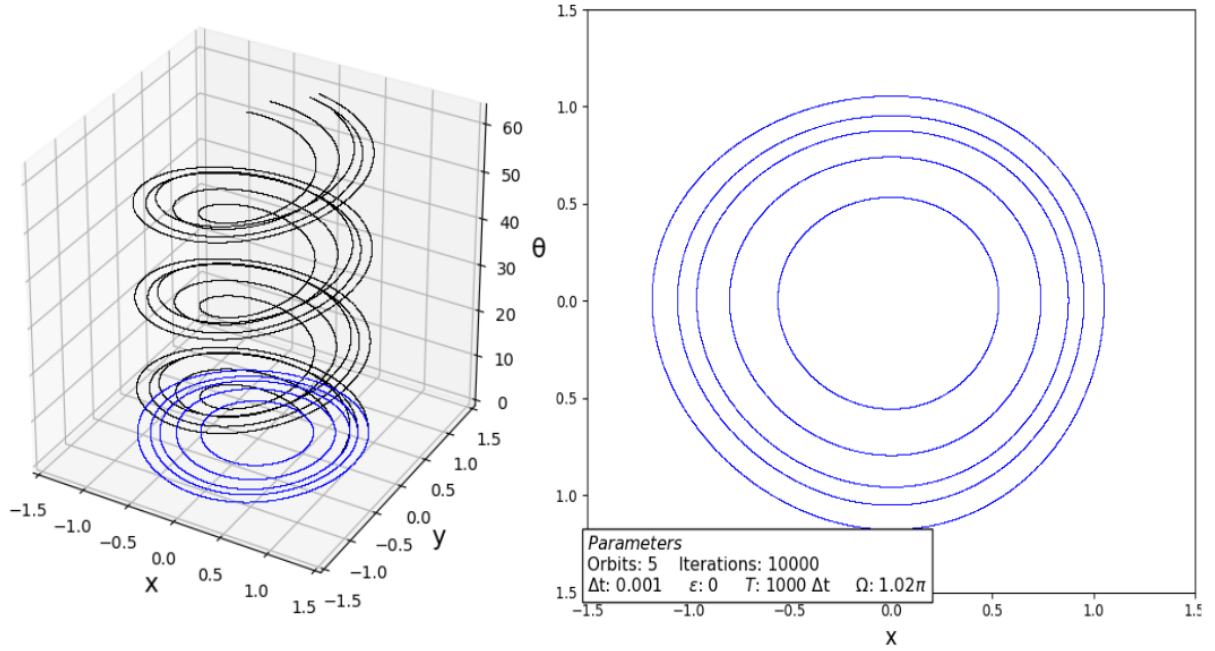


Figure 2.1: In the left figure is represented the map (2.14) in \mathbb{R}^3 and its projection onto the xy plane in blue. The map given in \mathbb{R}^2 by such a projection is shown on the right.

plane because in the original system that would be the plane of the orbits. In this 3 dimensional framework we apply the stroboscopic method that consist in sampling the trajectories at intervals equal to the period of the perturbation. In this case we define the stroboscopic map as

$$M_{Strob}(\mathbf{x}) = S_T(\mathbf{x}) = S_{2\pi}(\mathbf{x}) \quad (2.15)$$

where $S_t(x)$ is the continuous solution of the system $\dot{x} = \Phi(\mathbf{x})$ and $S_{\Delta t}(x)$ denotes the subset of points at a time distance Δt . The period T is 2π since the perturbation is sinusoidal.

In the figure (2.2) this procedure is shown in \mathbb{R}^3 together with its projection, for a perturbation amplitude $\epsilon = 0.1$. On the left column the full orbits are represented, while on the right the stroboscopic map is highlighted in red.

Recalling equations (2.14) note that θ is increased by $2\pi \frac{\Delta t}{T}$ each iteration, i.e. $\theta_n = \theta_0 + n2\pi \frac{\Delta t}{T}$. Choosing $\theta_0 = 0$, we have $\theta_n = 2\pi$ when $n\Delta t = T$. Thus setting the period as an integer multiple of the integration time interval, i.e. $T = k\Delta t$, the stroboscopic map is just a subset of the map (2.14), specifically it is the subsequence in which we take one point every k .

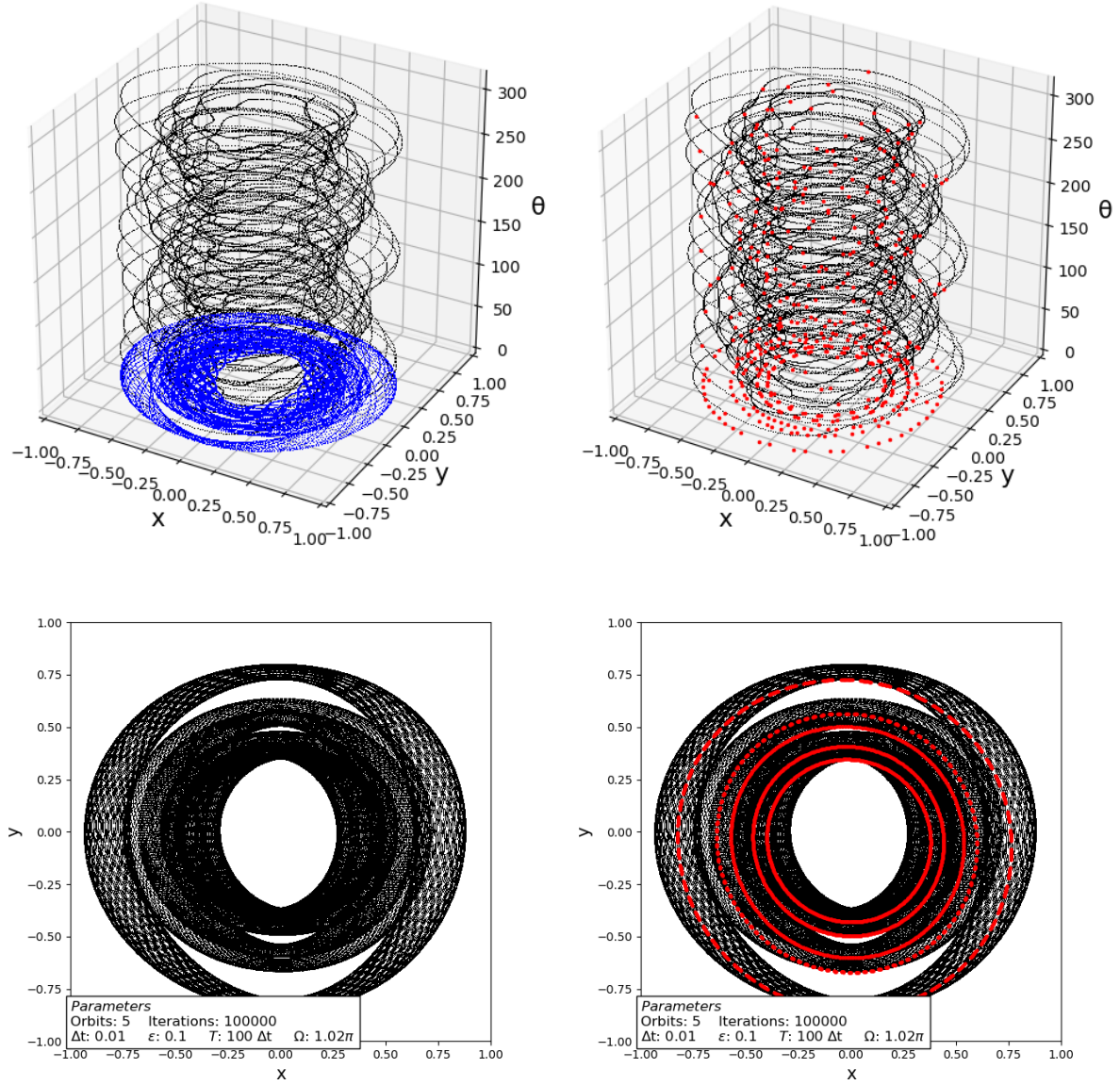


Figure 2.2: In the figures the trajectories in 3D and their xy projection are shown for a perturbation amplitude $\epsilon = 0.1$. On the right column the stroboscopic map is enlightened in red, together with its projection onto the plane. Note how more regular it is compared to the superimposition of all the orbits over time.

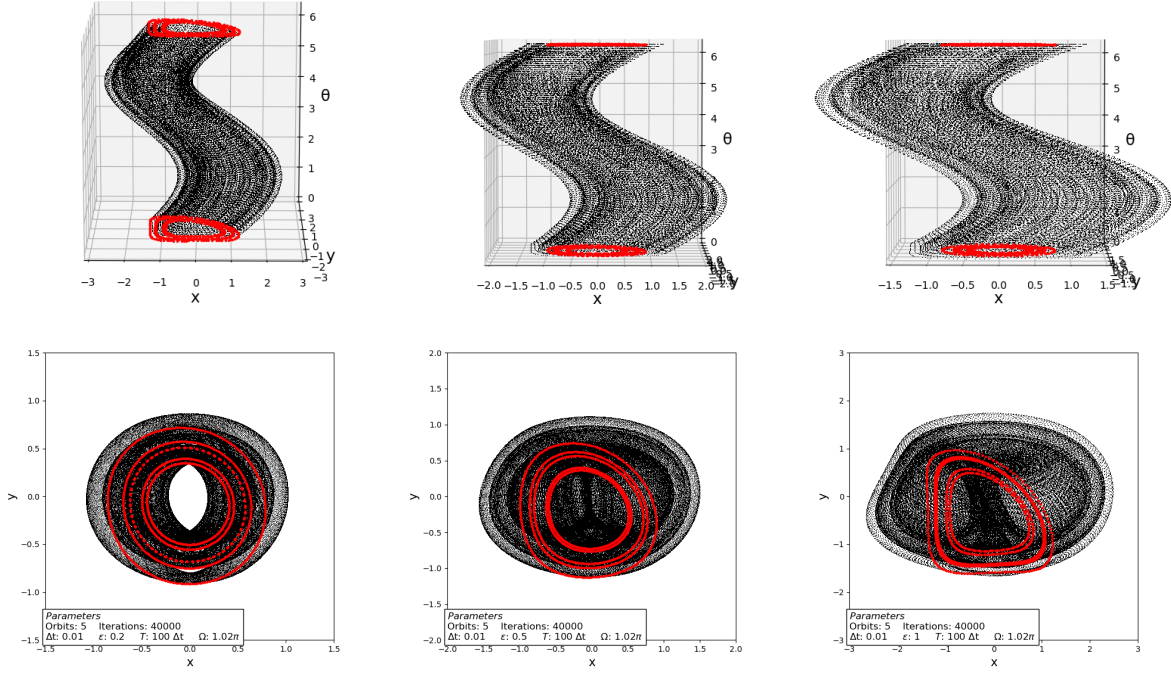


Figure 2.3: One period of the trajectories in 3D is shown in the top row, and their projection onto the xy plane in the bottom row. The noise have been set to 0.2 (left), 0.5 (center), and 1.0 (right). The stroboscopic map is shown in red.

We now give some insight on the effect of the perturbation, through the figure (2.3), in which the amplitude has been set to 0.2 (left), 0.5 (center) and 1 (right). The stroboscopic map is in any case enlightened in red. On the top row the evolution of the 3 dimensional system is shown, restricted to one period. The full orbit repeats over time the represented pattern. Note that the stroboscopic map in this case captures all the points at the top of the figure and that their projection onto the xy plane coincides with the orbits computed at the bottom, confirming the periodicity of the perturbation. The stroboscopic map shows the existence of an equilibrium that seems to be the only fixed point of the map. Increasing the amplitude of the perturbation causes the progressive deformation of the solutions and the displacement of the fixed point.

Finally some considerations are needed about the effect of the choice of the integration time. Since the map for $\epsilon = 0$ is symplectic the integration of the unperturbed system is good even for relatively large Δt . Therefore one of the key points is the resolution at which the single period is integrated, that can be expressed as a function of the parameter $\lambda := \frac{T}{\Delta t}$. In all the previous examples $\lambda = 100$ i.e. $T = 100\Delta t$ (this meaning that the stroboscopic map was the subset made up of one every 100 points of the whole map). Nevertheless the map does not depend solely on λ , since to each value of λ correspond an infinite set of couples of $(\Delta t, T)$ that indicate the balance between the resolution in the integration of the xy components and the resolution in the integration over the period of the perturbation.

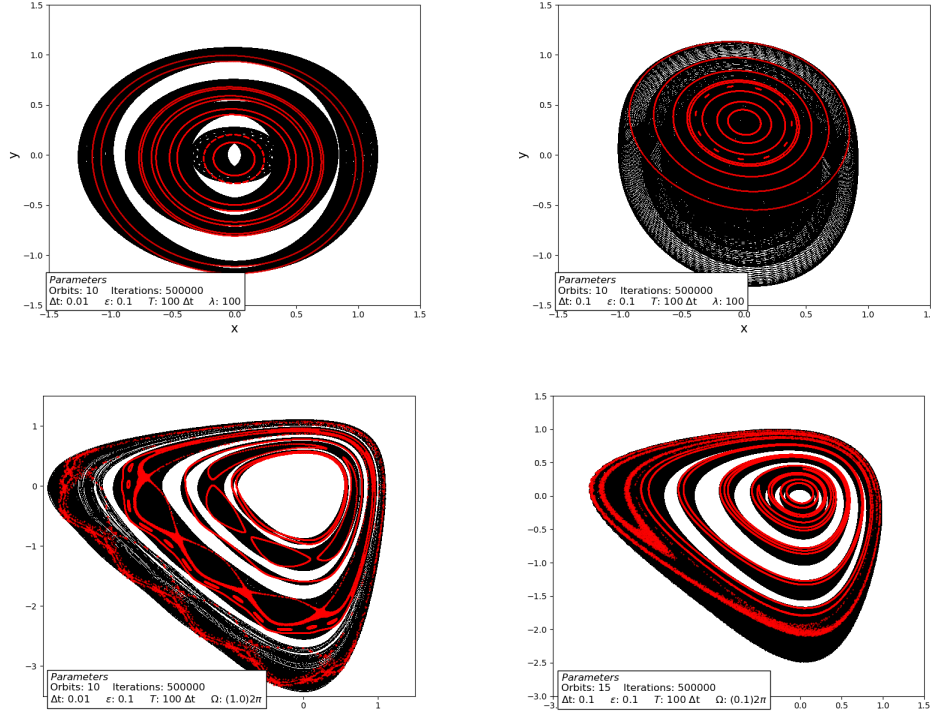


Figure 2.4: In the figures the stroboscopic map is shown in red, superimposed on the full orbit depicted in black. In the top row the evolution take place in the (x, y, θ) space using the map (2.13)-(2.14), while in the bottom row the orbits of the map (2.17)-(2.18) are represented, that gives the evolution in the (x, y, t) space. The comparison is useful since the resonance islands can be appreciated in the second row. Notice that all these cases have in common the factor λ indicating that the integration resolution for the period of perturbation is the same.

Different figures can appear in the phase space varying λ and Δt . To better show some features the integration have been made even with the following map, in which neither the scaling $(x, y) \mapsto \frac{(x, y)}{2\pi}$ nor the variable change $\theta = \omega t$ have been performed.

$$x_{n+1} = x_n + \Delta t(a^2 - e^{2y_{n+1}}) + \epsilon \Delta t \cos(\omega t_n) \quad (2.16)$$

$$y_{n+1} = y_n + \Delta t(e^{2x_n} - b^2) \quad (2.17)$$

$$t_{n+1} = t_n + \Delta t \quad (2.18)$$

Notable features of the map above include the compresence of chaotic and regular orbits, or the arise of chaos via resonance islands, even for small ϵ (figure (2.4)).

Orbits defined in the (x, y, θ) map, but diverging in the (x, y, t) space can happen, as the one represented in the figure (2.5). Notice that being $T = 2\Delta t$ the stroboscopic map is made up of one every two points of the complete map. This means that each two points a full period is closed, so $\Delta\theta = \pi$ and $\omega\Delta t = \frac{2\pi}{T}\Delta t = \pi$. In both cases the sequence given by the evaluation of the perturbation $\cos(\Delta\theta) = \cos(\omega\Delta t)$ is $+1, -1, +1, -1, \dots$

The difference in the evolution is due to the exponential terms of the maps. Expanding to the second order:

$$\Delta t(a^2 - e^{2y}) \simeq \Delta t(1 - (1 + 2y)) = -2\Delta t y = -y \quad (2.19)$$

$$\Delta t(a^2 - e^{y/\pi}) \simeq \Delta t(1 - (1 + \frac{y}{\pi})) = -\frac{\Delta t}{\pi} y \simeq -0.16y \quad (2.20)$$

recalling that $a=b=1$ and $\Delta t = 0.5$. In the second case the evolution is contracted.

Another notable point is that chaos can arise even in the (x, y, θ) map, for greater values of the amplitude, as in the figure (2.6, right column) in which $\epsilon = 0.5$. Note that even in this case, to regular orbits in the (x, y, θ) space correspond a resonance figure in the (x, y, t) space (figure (2.6, right column)).

The plot have been produced with Python with the code available here:

https://github.com/FMagnani/Stroboscopic_Map_Example

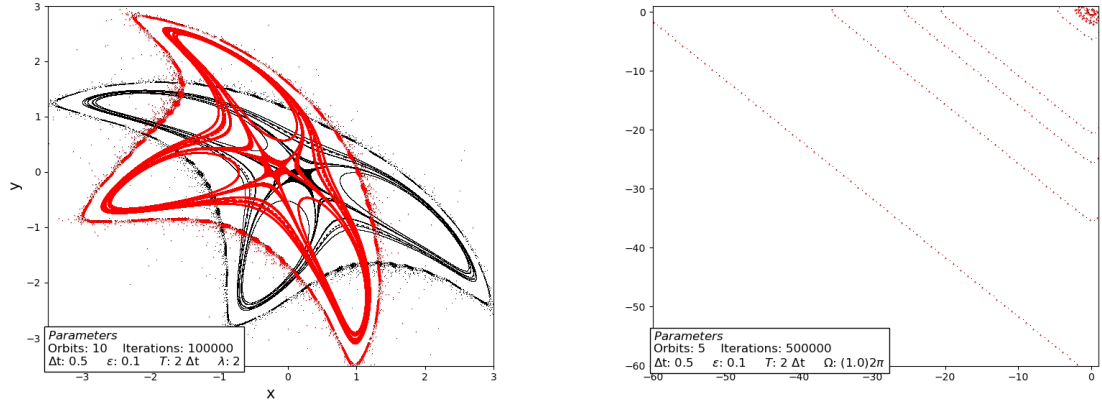


Figure 2.5: In both the figures the stroboscopic map is shown in red and the full map in black. Since the integration interval is half the period, the stroboscopic map is exactly one point every two of the complete map. On the left figure the evolution is computed in (x, y, θ) coordinates using the map (2.13)-(2.14) while on the right the orbits in xy are perturbed along time t , so using the map (2.17)-(2.18) defined in the (x, y, t) space.

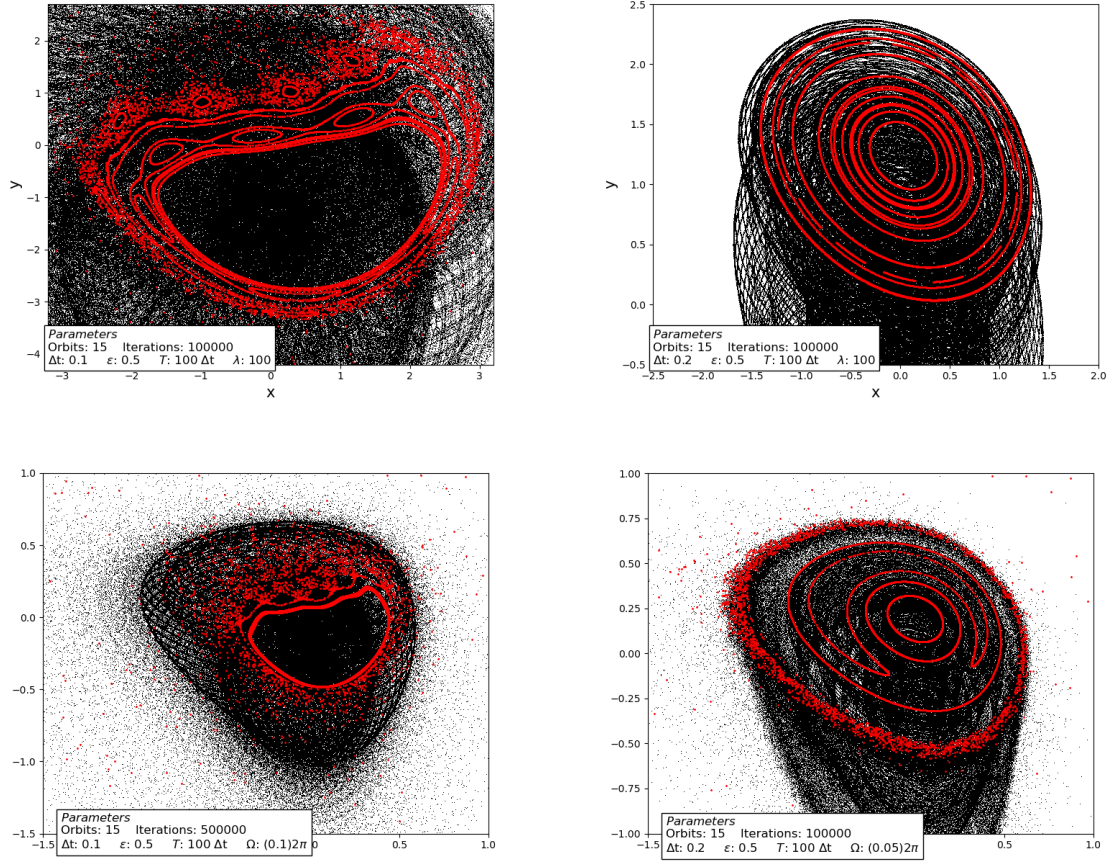


Figure 2.6: In the top row two cases are shown for the evolution of the system in coordinates (x, y, θ) while in the bottom row the evolution is computed in the (x, y, t) space. In both pairs of cases the amplitude of perturbation is $\epsilon = 0.5$. On the left column the transition from regular to mixed to purely chaotic behaviour happens for both the maps. The right column shows how regular orbits on the (x, y, θ) space can map to chaotic orbits and resonance figures in the (x, y, t) space.